Metal–Organic Composites

DOI: 10.1002/anie.201006882

Cooperative Assembly of Three-Ring-Based Zeolite-Type Metal–Organic Frameworks and Johnson-Type Dodecahedra**

*Shou-Tian Zheng, Fan Zuo, Tao Wu, Burcin Irfanoglu, Chengtsung Chou, Ruben A. Nieto, Pingyun Feng, and Xianhui Bu**

Large-scale industrial applications of zeolites in areas such as air separation and petrochemical processing have rendered the zeolite-type topology a prime target in new materials design.[1] Zeolite structure types exemplified by commercially important zeolites A, X, and ZSM-5 are characterized by 4-connected open topologies and TL_2 framework compositions (T indicates tetrahedral, and L is a bicoordinated species between two T atoms). During the past decades, the synthesis of zeolite-type MOFs,[2–13] defined here as metal–organic frameworks (MOFs) with zeolite-type 4-connected topologies, has attracted increasing interest.

Known zeolite-type MOFs are mostly synthesized by a strategy based on the mimicking of the Si-O-Si bond angle of approximately 145° by T-L-T angles in MOFs through judicious choice of metal and ligand geometry. This strategy has led to the preponderance of imidazolate-type ligands (with or without auxiliary functional groups such as COO^-) in zeolite-type MOF chemistry,[3–4,7–11] while "pure" carboxylates (those with only COO^- donor groups) that permeate most other aspects of MOF chemistry have played a small role in the design of zeolite-type MOFs, possibly because of their perceived "wrong" T-L-T angles.

On the other hand, it has long been recognized that zeolite-type nets can accommodate a large range of T-O-T angles. For example, in gallosilicates, gallogermanates, and zincoarsenates, an increase in the T–O bond length (compared to silicates) leads to a decrease in the T-O-T angle to as low as 123.8° in a zincoarsenate sodalite.[14] Furthermore, the longer T–O distance and the correspondingly smaller T-O-T angle also provide some advantages, because they contribute to the formation of new topologies and also help to stabilize secondary building units (SBUs, e.g., three-rings) that are strained and difficult to form in silicates.[15]

In developing strategies for constructing new porous materials, the three-ring, which has the smallest possible ring size, is one of the most desirable SBUs because it can help to create new topological types with low framework density[3b,16] and could also induce the concurrent formation of large ring sizes such as 14-rings. (The ring size refers to the number of T nodes in a ring, and the smallest ring size in known zeolite structure types is rarely three, often four, and sometimes five.)[2c] Additionally, the three-ring is also one of the most effective SBUs for constructing metal–organic polyhedra (MOPs).[17–19] For example, three out of five Platonic solids and nine out of 13 Archimedean solids contain triangles. Yet, three-rings are uncommon in both traditional porous oxides and more recent MOFs.[2c]

Thus, it becomes clear that the introduction of three-rings could allow access to new zeolite-like MOFs and MOPs. Herein, we select In^{3+} ions as metal centers and mixed dicarboxylic linkers with 120 and 180° angles as complementary and cooperative linkers for the construction of three-ring-based zeolite-type nets (Scheme 1) and MOPs. Among metal ions, In^{3+} is of special interest, because it can form a four-connected $\{In(O_2CR)_4\}$ group, which is an appealing T node for targeting zeolite-type MOFs and MOPs.[12,13] Dicarboxylic linkers with 120° bend angle are chosen because of their ability to induce the assembly of In_3 three-rings. The second dicarboxylic linker is chosen to provide the cross-links between three-rings to generate an overall 3D architecture. Using this strategy, we have been able to synthesize not only a series of isostructural three-ring-based zeolite-type MOFs

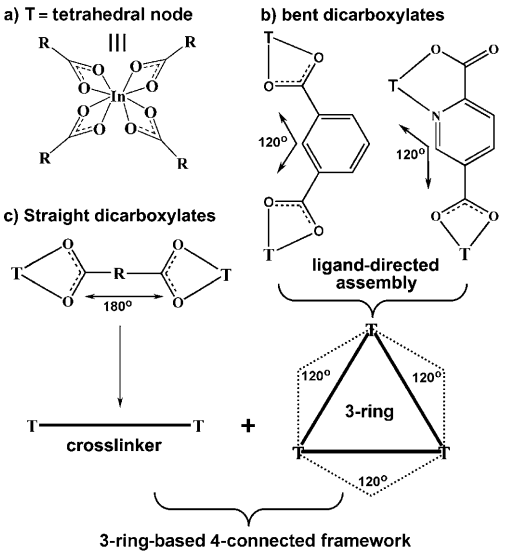

Scheme 1. Synthetic strategy for the construction of three-ring-based zeolite nets using two symmetry-complementary ligands.

[*] Dr. S.-T. Zheng, B. Irfanoglu, C. Chou, R. A. Nieto, Prof. Dr. X. Bu
Department of Chemistry and Biochemistry
California State University, Long Beach
1250 Bellflower Boulevard, Long Beach, CA 90840 (USA)
Fax: (+1) 562-985-8557
E-mail: xbu@csulb.edu
F. Zuo, T. Wu, Prof. Dr. P. Feng
Department of Chemistry, University of California
Riverside, CA 92521 (USA)

[**] We thank the NSF (X.B. DMR-0846958, P.F. DMR-0907175) and DOE (P.F. DE-SC0002235) for support of this work. X.B. is a Henry Dreyfus Teacher Scholar.

Supporting information for this article is available on the WWW under http://dx.doi.org/10.1002/anie.201006882.

Table 1: Summary of crystal data and refinement results.[a]

Compound	Formula	Space group	*a* [Å]	*b* [Å]	*c* [Å]	α [°]	β [°]	γ [°]	*R*(F)
CPM-2-NH_2	$[N(CH_3)_2]_3[In_3(aip)_3(bpdc)_3]$·solvent	*P*31*c*	27.2959(7)	27.2959(7)	28.0896(16)	90	90	120	0.0852
CPM-2-OH	$[N(CH_3)_2]_3[In_3(hip)_3(bpdc)_3]$·solvent	*P*31*c*	27.6060(32)	27.6060(32)	28.1798(41)	90	90	120	[b]
CPM-2-H	$[N(CH_3)_2]_3[In_3(m\text{-}bdc)_3(bpdc)_3]$·solvent	*P*31*c*	27.2959(30)	27.2959(30)	28.0896(55)	90	90	120	[b]
CPM-2-NH_2-Cs	$Cs[N(C_2H_5)_2]_2[In_3(aip)_3(bpdc)_3]$·solvent	*P*31*c*	27.3449(3)	27.3449(3)	28.2554(7)	90	90	120	0.082
CPM-3	$[N(CH_3)_2]_3[In_3(aip)_3(sdc)_3]$·solvent	*P*31*c*	27.2340(2)	27.2340(2)	32.8706(7)	90	90	120	0.0946
CPM-8	$[N(CH_3)_2]_{10}[In_{10}(pdc)_{16}(bpdc)_4]$·solvent	$P2_1/c$	22.5221(10)	29.1986(12)	32.0959(11)	90	132.243(2)	90	0.1040
CPM-9	$[N(CH_3)_2]_{10}[In_{10}(pdc)_{16}(ndc)_4]$·solvent	*Pcca*	39.7134(7)	17.4359(3)	46.3618(8)	90	90	90	0.0963

[a] H_2bpdc = 4,4′-biphenyldicarboxylic acid; H_2hip = 5-hydroxyisophthalic acid; H_2aip = 5-aminoisophthalic acid; *m*-H_2bdc = 1,3-benzenedicarboxylic acid; H_2sdc = 4,4′-stilbenedicarboxylic acid; H_2pdc = pyridine-2,5-dicarboxylic acid; H_2ndc = naphthalene-1,4-dicarboxylic acid. [b] The unit cells of CPM-2-OH and CPM-2-H were obtained by single-crystal X-ray diffraction. The bulk samples of CPM-2-OH and CPM-2-H were identified as isostructural to CPM-2-NH_2 using XPRD (Figure S6 in the Supporting Information).

(denoted as CPM-2-NH_2, CPM-2-OH, CPM-2-H, CPM-2-NH_2-Cs, and CPM-3) with large 12-ring pore size (Table 1, CPM = crystalline porous material), but also two Johnson-type MOPs (denoted as CPM-8 and CPM-9) with elongated square bipyramidal configuration.

CPM-2-NH_2 crystallizes in a highly symmetric and yet noncentrosymmetric trigonal space group *P*31*c*. The asymmetric unit (Figure S1 in the Supporting Information) consists of three crystallographically independent In^{3+} ions, each of which is coordinated by four bidentate chelating carboxylate groups from two 5-aip and two bpdc ligands to form a T node. These three indium sites exhibit only one type of loop configuration (Figure 1a) involving one three-ring corresponding to a triangular $\{In_3(aip)_3\}$ group (Figure 1b). The loop configuration is a simple graph showing how many three- or four-membered rings a given T node is involved in.[2c] The triangular $\{In_3(aip)_3\}$ groups act as SBUs, and each of them is connected to six neighboring ones through six linear bpdc ligands (Figure 1c), resulting in the formation of a 3D framework with the zeolite NPO topology (Figure 1d) originally discovered in a nitridophosphate.[2c,20]

CPM-2-NH_2 exhibits two types of infinite channels along the *c* axis. The first type has small three-ring openings that can accommodate a sphere with a maximum free diameter of 4.6 Å. The three-ring channel consists of one kind of nonanuclear $\{In_9(aip)_6(bpdc)_6\}$ cage built from two $\{In_3(aip)_3\}$

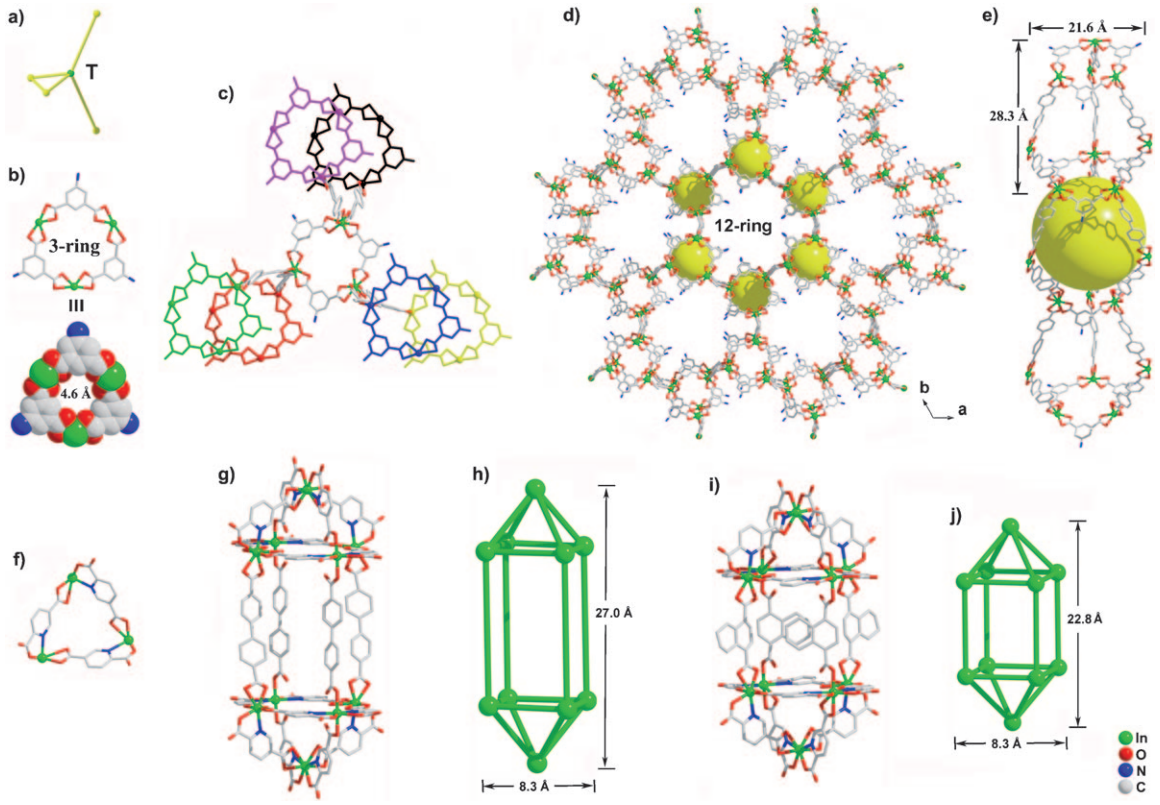

Figure 1. a) View of the loop configuration in CPM-2-NH_2. b) Structure of the $\{In_3(aip)_3\}$ three-ring. c) Coordination of the $\{In_3(aip)_3\}$ three-ring to adjacent units. d,e) 3D view of the NPO-zeolite framework and nonanuclear $\{In_9(aip)_6(bpdc)_6\}$ cages, respectively. f) Structure of the $\{In_3(pdc)_3\}$ three-ring. g,h and i,j) Schematic representations of the MOPs in CPM-8 and CPM-9, respectively.

three-rings linked by three {In(bpdc)$_2$} groups (Figure 1e). The free diameter of the largest sphere that can fit into the cage is approximately 14.6 Å. By sharing three-ring faces, adjacent cages are joined together to form infinite three-ring channels. Interestingly, arrays of three-ring channels form a hexagonal pattern and are interconnected through linear bpdc linkers to generate a 12-ring channel (Figure 1d). It is worth noting that unlike zeolites in which the aperture size is primarily determined by the ring size (i.e., the number of T nodes), the aperture size in MOFs is generally determined by the ligand length. Zeolite-type MOFs with large ring sizes such as 12-rings are rare.[11] In CPM-2-NH_2, the narrowest free diameter in the 12-ring channel is 12.2 Å (Figure S2 in the Supporting Information).

In contrast to zeolite-type MOFs that rely on heterocyclic ligands (e.g., imidazole derivatives), CPM-2-NH_2 is based on a pure metal carboxylate framework with only COO^- donors. To date, zeolite-type MOFs with pure metal carboxylate frameworks remain rare. Compared with heterocyclic ligands such as imidazolates, pure dicarboxylates usually have longer distances between donor sites, which helps to increase the separation between adjacent T nodes. As a result, the framework density (FD; 0.33) of a single sublattice in CPM-2-NH_2 is very low compared to known zeolite-type MOFs (usually larger than 2.0) and inorganic zeolites (usually larger than 10.0). The FD is defined as the number of T nodes per 1000 Å^3.[2c] Such an open net, however, resulted in the formation of a three-fold interweaving structure in CPM-2 (Figure S3 in the Supporting Information). Still, the overall structure is quite open, with a total guest-accessible volume of 44% (8074 Å^3 per unit cell). Even considering all triply interweaving nets, the overall FD (1.0) is still very low.

The presence of two symmetry-complementary ligands in CPM-2-NH_2 makes it possible to tune the framework composition by replacing either one of two ligands. By using two other bent dicarboxylates (i.e., 5-hip and 1,3-bdc), two more phases (denoted CPM-2-OH and CPM-2-H) were obtained. The functional groups (NH_2^- and OH^-) in these structures are oriented towards the pore center of 12-ring channels and can lead to different interactions with guest molecules. Alternatively, the bpdc ligand that cross-links three-rings can also be replaced by other linear dicarboxylates. For example, the use of a longer linear dicarboxylate H_2sbc leads to CPM-3 with a guest-accessible volume of 11270 Å^3 per unit cell (53.4%). It is also possible to introduce inorganic cations (i.e., Cs^+) into the pore space through direct synthesis by simply including a cesium source (e.g., CsCl) into the synthesis mixture with diethylformamide (DEF) as the solvent, leading to a Cs-containing phase, denoted as CPM-2-NH_2-Cs.

We then further examined the versatility of our synthetic method by expanding from the bent carboxylate system to the bent heterocyclic carboxylate system. We selected H_2pdc with a 120° bend angle, and ligands for cross-linking three-rings are bpdc and 1,4-ndc (Table 1). The combination of two symmetry-complementary ligands led to two discrete three-ring-based MOPs, denoted as CPM-8 and CPM-9.

As shown in Figure 1 f–j, CPM-8 and CPM-9 consist of ten In^{3+} ions, sixteen bent pdc, and four linear bpdc (or 1,4-ndc) ligands. The presence of pdc with a 120° bend angle induces the formation of a basic {In_3(pdc)$_3$} three-ring SBU (Figure 1f) and subsequently a pentanuclear square pyramidal {In_5(pdc)$_8$} cluster. In the presence of the symmetry-complementary dicarboxylates, two pentanuclear pyramidal moieties are pillared into an expanded size-tunable cage structure comprising eight triangular and four quadrilateral windows (Figure 1g). With four linear bpdc ligands, the dimensions of CPM-8 are approximately $8.3 \times 8.3 \times 27.0$ Å (atom-to-atom distance). With a shorter ndc ligand, an analogous decanuclear indium MOP CPM-9, $8.3 \times 8.3 \times 22.8$ Å in dimension, was obtained.

When indium ions are viewed as vertices and the ligands as edges, CPM-8 and CPM-9 can be described as elongated square bipyramids (Figure 1h,j), which are Johnson solids. To date, a number of MOPs with various sizes and shapes have been reported.[16–18] However, most known MOPs are Archimedean or Platonic solids in which all the vertices are identical. In comparison, Johnson solids possess different kinds of vertices.[17a]

Thermal gravimetric analysis of CPM-2-NH_2 shows that the removal of solvent molecules occurs in the temperature range 60 to approximately 220 °C (Figure S4 in the Supporting Information). PXRD further confirms that the desolvated sample retains its crystallinity up to about 250 °C (Figure S5 in the Supporting Information). The UV/Vis diffuse reflectance spectrum of CPM-2-NH_2 shows that its band gap is 3.0 eV (Figure S7 in the Supporting Information). Photocatalytic H_2 production experiments were conducted in a sealed circulation system. Platinum (1%) was loaded as a cocatalyst by UV irradiation of an aqueous $PtCl_4$ solution. In a typical run, sample (0.100 g) was suspended in 25% methanol aqueous solution (120 mL, containing 0.0017 g $PtCl_4$) under magnetic stirring. Then the mixture was irradiated with a 300 W xenon lamp for 30 min, which led to the deposition of the Pt nanoparticles onto the sample surface as cocatalyst. After degassing the system for one hour, the 300 W xenon lamp was applied to execute the photocatalytic reaction. The products were analyzed by gas chromatography using an instrument (Shimadzu GC-8A) equipped with a thermal conductivity detector (TCD). As shown in Figure S8 in the Supporting Information, the photocatalytic reactions of CPM-2-NH_2 exhibit a stable H_2 release rate of 2.0 μmol h^{-1} per 0.1 g, thus demonstrating that the sample has photocatalytic activity for the generation of H_2 gas from water under UV irradiation. The photocatalytic activity of CPM-2-NH_2 compares favorably with that of the In_2O_3 powder, which gave a dihydrogen release rate of 2 μmol h^{-1} per 0.3 g under the irradiation of 500 W high-pressure mercury lamp.[21]

In summary, the utilization of bent dicarboxylates for directing the formation of three-rings and linear dicarboxylates for cross-linking three-rings has allowed the synthesis of three-ring-based zeolite-type MOFs and MOPs with tunable framework and extraframework compositions. These new materials possess structural and topological features (such as three-rings, large 12-ring channels, and expanded MOP cages) that are the direct results of the synthetic strategy. The synthesis of CPM-2 and CPM-3 shows a new pathway for the creation of zeolite-type MOFs using

only carboxylate functionality, instead of the currently popular practices that rely on heterocyclic compounds. CPM-8 and CPM-9 are indium-based metal–organic polyhedra and belong to a family of Johnson-type solids that are uncommon among MOPs. As demonstrated by CPM-2-NH_2, these materials behave as semiconductors and can function as photocatalysts for the generation of dihydrogen from water.

Received: November 3, 2010
Published online: January 21, 2011

Keywords: mixed ligands · organic–inorganic hybrid composites · water splitting · zeolites

[1] a) H. Van Bekkum, E. M. Flanigen, P. A. Jacobs, J. C. Jansen, *Introduction to Zeolite Science and Practice*, Elsevier, Amsterdam, **2001**; b) R. E. Morris, *Top. Catal.* **2010**, *53*, 19; c) E. R. Parnham, R. E. Morris, *Acc. Chem. Res.* **2007**, *40*, 1005.

[2] a) G. Férey, C. Serre, F. Millange, S. Surble, J. Dutout, I. Margiolaki, *Angew. Chem.* **2004**, *116*, 6456; *Angew. Chem. Int. Ed.* **2004**, *43*, 6296; b) Q. Fang, G. Zhu, M. Xue, J. Sun, Y. Wei, S. Qiu, R. Xu, *Angew. Chem.* **2005**, *117*, 3913; *Angew. Chem. Int. Ed.* **2005**, *44*, 3845; c) A. C. Baerlocher, L. B. McCusker, D. H. Olson, *Atlas of Zeolite Framework Types*, 6th ed, Elsevier, Amsterdam, **2007**.

[3] a) X. C. Huang, Y. Y. Lin, J. P. Zhang, X. M. Chen, *Angew. Chem.* **2006**, *118*, 1587; *Angew. Chem. Int. Ed.* **2006**, *45*, 1557; b) T. Wu, X. Bu, R. Liu, Z. Lin, J. Zhang, P. Feng, *Chem. Eur. J.* **2008**, *14*, 7771 – 7773.

[4] a) K. S. Park, Z. Ni, A. P. Côté, J. Y. Choi, R. Huang, F. J. Uribe-Romo, H. K. Chae, M. O'Keeffe, O. M. Yaghi, *Proc. Natl. Acad. Sci. USA* **2006**, *103*, 10186; b) Y. Q. Tian, Y. M. Zhao, Z. X. Chen, G. N. Zhang, L. H. Weng, D. Y. Zhao, *Chem. Eur. J.* **2007**, *13*, 4146.

[5] X. D. Guo, G. S. Zhu, Z. Y. Li, Y. Chen, X. T. Li, S. L. Qiu, *Inorg. Chem.* **2006**, *45*, 4065.

[6] Y. Liu, V. C. Kravtsov, R. Larsen, M. Eddaoudi, *Chem. Commun.* **2006**, 1488.

[7] H. Hayashi, A. P. Côté, H. Furukawa, M. O'Keeffe, O. M. Yaghi, *Nat. Mater.* **2007**, *6*, 501.

[8] T. Wu, X. Bu, J. Zhang, P. Feng, *Chem. Mater.* **2008**, *20*, 7377.

[9] R. Banerjee, A. Phan, B. Wang, C. Knobler, H. Furukawa, M. O'Keeffe, O. M. Yaghi, *Science* **2008**, *319*, 939.

[10] W. Morris, C. J. Doonan, H. Furukawa, R. Banerjee, O. M. Yaghi, *J. Am. Chem. Soc.* **2008**, *130*, 12626.

[11] R. Banerjee, H. Furukawa, D. Britt, C. Knobler, M. O'Keeffe, O. M. Yaghi, *J. Am. Chem. Soc.* **2009**, *131*, 3875.

[12] a) F. Nouar, J. Eckert, J. F. Eubank, P. Forster, M. Eddaoudi, *J. Am. Chem. Soc.* **2009**, *131*, 2864; b) M. H. Alkordi, J. A. Brant, L. Wojtas, V. C. Kravtsov, A. J. Cairns, M. Eddaoudi, *J. Am. Chem. Soc.* **2009**, *131*, 17753.

[13] S. Huh, T. Kwon, N. Park, S. Kimc, Y. Kim, *Chem. Commun.* **2009**, 4953.

[14] T. M. Nenoff, W. T. A. Harrison, T. E. Gier, N. L. Keder, C. M. Zaremba, V. I. Srdanov, J. M. Nicol, G. D. Stucky, *Inorg. Chem.* **1994**, *33*, 2472.

[15] X. Bu, P. Feng, T. E. Gier, D. Zhao, G. D. Stucky, *J. Am. Chem. Soc.* **1998**, *120*, 13389.

[16] a) J. Jiang, J. L. Jorda, M. J. Diaz-Cabanas, J. Yu, A. Corma, *Angew. Chem.* **2010**, *122*, 5106; *Angew. Chem. Int. Ed.* **2010**, *49*, 4986; b) A. Corma, M. J. Díaz-Cabañas, J. Jianga, M. Afeworki, D. L. Dorset, S. L. Soled, K. G. Strohmaier, *Proc. Natl. Acad. Sci. USA* **2010**, *107*, 13997.

[17] a) S. R. Seidel, P. J. Stang, *Acc. Chem. Res.* **2002**, *35*, 972; b) D. J. Tranchemontagne, Z. Ni, M. O'Keeffe, O. M. Yaghi, *Angew. Chem.* **2008**, *120*, 5214; *Angew. Chem. Int. Ed.* **2008**, *47*, 5136; c) H. Furukawa, J. Kim, N. W. Ockwig, M. O'Keeffe, O. M. Yaghi, *J. Am. Chem. Soc.* **2008**, *130*, 11650; d) J. J. Perry IV, J. A. Perman, M. J. Zaworotko, *Chem. Soc. Rev.* **2009**, *38*, 1400.

[18] a) J. R. Li, H. C. Zhou, *Angew. Chem.* **2009**, *121*, 8617; *Angew. Chem. Int. Ed.* **2009**, *48*, 8465; b) J. R. Li, D. J. Timmons, H. C. Zhou, *J. Am. Chem. Soc.* **2009**, *131*, 6368; c) D. F. Sava, V. C. Kravtsov, J. Eckert, J. F. Eubank, F. Nouar, M. Eddaoudi, *J. Am. Chem. Soc.* **2009**, *131*, 10394; d) Z. Lu, C. B. Knobler, H. Furukawa, B. Wang, G. Liu, O. M. Yaghi, *J. Am. Chem. Soc.* **2009**, *131*, 12532; e) T. Ahnfeldt, N. Guillou, D. Gunzelmann, I. Margiolaki, T. Loiseau, G. Férey, J. Senker, N. Stock, *Angew. Chem.* **2009**, *121*, 5265; *Angew. Chem. Int. Ed.* **2009**, *48*, 5163; f) M. B. Duriska, S. M. Neville, J. Lu, S. S. Iremonger, J. F. Boas, C. J. Kepert, S. R. Batten, *Angew. Chem.* **2009**, *121*, 9081; *Angew. Chem. Int. Ed.* **2009**, *48*, 8919.

[19] a) Q. F. Sun, J. Iwasa, D. Ogawa, Y. Ishido, S. Sato, T. Ozeki, Y. Sei, K. Yamaguchi, M. Fujita, *Science* **2010**, *328*, 1144; b) K. Suzuki, K. Takao, S. Sato, M. Fujita, *J. Am. Chem. Soc.* **2010**, *132*, 2544; c) J. R. Li, H. C. Zhou, *Nat. Chem.* **2010**, *2*, 893; d) M. Jaya Prakash, M. Oh, X. Liu, K. N. Han, G. H. Seong, M. S. Lah, *Chem. Commun.* **2010**, *46*, 2049.

[20] S. Correll, O. Oeckler, N. Stock, W. Schnick, *Angew. Chem.* **2003**, *115*, 3674; *Angew. Chem. Int. Ed.* **2003**, *42*, 3549.

[21] S. Sato, *J. Photochem. Photobiol. A* **1988**, *45*, 361.

